Correlation Analysis of Earthquake Intensity Measures and Engineering Demand Parameters of Reactor Containment Structure

Xuan-Hung Vu
Department of Civil Engineering, Vinh University
Vinh, Vietnam
vxhlkc@gmail.com

Thanh-Tung Thi Nguyen
Department of Civil Engineering, Vinh University
Vinh, Vietnam
ntttung@gmail.com

Van-Long Phan
Department of Civil Engineering, Vinh University
Vinh, Vietnam
phanlongkxd@vinhuni.edu.vn

Duy-Duan Nguyen
Department of Civil Engineering, Vinh University
Vinh, Vietnam
duyduankxd@vinhuni.edu.vn

Abstract-This study aims to analyze the correlation between earthquake Intensity Measures (IMs) and seismic responses of a reactor containment building in an APR-1400 nuclear power plant. A total of 20 IMs were employed to develop Seismic Demand Regression Models (SDRMs), which show the relationship between IMs and engineering demand parameters. A numerical model of the structure was constructed using the Lumped-Mass Stick Model (LMSM) in SAP2000. Additionally, a three-dimensional finite element model was developed to validate the simplified LMSM approach. A set of 90 ground motion records was used to perform a time-history analysis, where the motions cover a wide range of amplitude, intensity, epicenter distance, significant duration, and frequency of earthquakes. Engineering demand parameters were monitored in terms of floor accelerations and displacements. Consequently, strongly correlated IMs were identified based on the evaluation of SDRMs using four statistical indicators: coefficient of determination, standard deviation, practicality, and proficiency. The results showed that the strongest IMs were Sa(T1), Sv(T1), and Sd(T1) followed by ASI, EPA, PGA, and A95. On the other hand, the weakly correlated IMs were PGD, DRMS, SED, VRMS, PGV, HI, VSI, and SMV.

Keywords-reactor containment structure; earthquake intensity measure; seismic demand regression model; floor acceleration; floor displacement

I. INTRODUCTION

Currently, seismic design codes and guidelines use Peak Ground Acceleration (*PGA*) and Spectral Acceleration (S_a) as intensity measures. These parameters are widely employed to evaluate the probabilistic seismic damage of structures. However, each structure has specific characteristics, such as structural dimensions, material properties, and details. Therefore, the correlation between seismic structural responses and earthquake intensity measures may differ for different structure types. Numerous studies evaluated the correlation between seismic Intensity Measures (IMs) and responses of different structures such as buildings [1-6], bridges [7-12], intake tanks [13], chimneys [14], and underground structures [15-17]. These studies concluded that *PGA* and S_a were not the optimal parameters to evaluate seismic responses and fragility analyses of structures. There is a need to systematically identify efficient earthquake IMs for seismic risk analysis of Nuclear Power Plants (NPPs), where the reactor containment building is one of the crucial structures.

Some studies investigated the interrelation of the responses of NPP structures and earthquake IMs. In [23], the correlation coefficients between typical IMs and seismic fragility of the Canada Deuterium Uranium reactor building were determined, pointing out that spectral acceleration $S_a(T_1)$ and spectral displacement at the fundamental period $S_d(T_1)$ are the most correlated IMs. In [24], time-history analysis was performed to recognize the strongly correlated earthquake IMs with the structural responses of base-isolated nuclear power plant structures, considering the high-frequency content of earthquakes. As a result, *PGA*, *A95*, and Sustained Maximum Acceleration (*SMA*) had the largest correlation with structural behaviors subjected to low-frequency earthquakes. Meanwhile, Specific Energy Density (*SED*), Characteristic Intensity (I_c), and Arias Intensity (I_a) were the strongest IMs under high-frequency ground motions. However, a systematic study on the correlation analysis between seismic IMs and structural behaviors of the 1400 NPP containment structure has not been performed. Since this structure is designed according to the US Nuclear Regulation Commission 1.60 (NRC 1.60) with *PGA*=0.3g, a selection of large ground motions is required, where the mean spectrum matches the design.

Moreover, a simplified numerical model called the Lumped Mass Stick Model (LMSM) and a full Three-Dimensional

---

Corresponding author: Duy-Duan Nguyen

Finite Element Model (3D FEM) have been used to evaluate nuclear structures [18]. However, since 3D FEM takes a long time for time-history analysis and occupies a large amount of memory, LMSM is preferred. Several studies demonstrated that LMSM was capable of evaluating fragility analyses of NPP structures [19-22]. This study conducted a correlation analysis between IMs and Engineering demand Parameters (EDPs) of reactor containment structures. A total of 20 IMs were considered to establish seismic demand regression models representing the relationship between IMs and EDPs. A numerical model of the containment structure was developed using the simplified LMSM in SAP2000. Additionally, a solid-based 3D FEM was built to validate the LMSM. A set of 90 seismic ground motion records was selected for time-history analysis. The EDPs were measured in terms of floor accelerations and displacements. Four statistical properties were used to evaluate the efficiency of seismic demand regression models, including coefficient of determination (R^2), standard deviation, practicality, and proficiency.

II. EARTHQUAKE INTENSITY MEASURES AND INPUT GROUND MOTIONS

This study selected 20 IMs to develop the seismic demand regression models, as shown in Table I. These IMs were classified in by amplitude, frequency, intensity, and energy.

TABLE I.   CONSIDERED EARTHQUAKE INTENSITY MEASURES

No	Earthquake IMs	Formula	Unit	Ref.
1	Peak ground acceleration	PGA = max |a(t)|	g	-
2	Peak ground velocity	PGV = max |v(t)|	m/s	-
3	Peak ground displacement	PGD = max |d(t)|	m	-
4	Root-mean-square of acceleration	$A_{rms} = \sqrt{\frac{1}{t_{tot}}\int_0^{t_{tot}} a(t)^2 dt}$	g	[25]
5	Root-mean-square of velocity	$V_{rms} = \sqrt{\frac{1}{t_{tot}}\int_0^{t_{tot}} v(t)^2 dt}$	m/s	[25]
6	Root-mean-square of displacement	$D_{rms} = \sqrt{\frac{1}{t_{tot}}\int_0^{t_{tot}} d(t)^2 dt}$	m	[25]
7	Arias intensity	$I_a = \frac{\pi}{2g}\int_0^{t_{tot}} a(t)^2 dt$	m/s	[26]
8	Characteristic intensity	$I_c = (A_{rms})^{2/3}\sqrt{t_{tot}}$	$m^{1.5}/s^{2.5}$	[27]
9	Specific energy density	$SED = \int_0^{t_{tot}} v(t)^2 dt$	m^2/s	-
10	Cumulative absolute velocity	$CAV = \int_0^{t_{tot}} |a(t)| dt$	m/s	[28]
11	Acceleration spectrum intensity	$ASI = \int_{0.1}^{0.5} S_a(\xi = 0.05, T) dT$	g*s	[29]
12	Velocity spectrum intensity	$VSI = \int_{0.1}^{2.5} S_v(\xi = 0.05, T) dT$	m	[29]
13	Housner spectrum intensity	$HI = \int_{0.1}^{2.5} PS_v(\xi = 0.05, T) dT$	m	[30]
14	Sustained maximum acceleration	SMA = the 3rd of PGA	g	[31]
15	Sustained maximum velocity	SMV = the 3rd of PGV	m/s	[31]
16	Effective peak acceleration	$EPA = \frac{mean(S_a^{0.1-0.5}(\xi=0.05))}{2.5}$	g	[28]
17	Spectral acceleration at T_1	$S_a(T_1)$	g	[32]
18	Spectral velocity at T_1	$S_v(T_1)$	m/s	-
19	Spectral displacement at T_1	$S_d(T_1)$	m	-
20	A95 parameter	$A_{95} = 0.764\, I_a^{0.438}$	g	[33]

A group of 90 ground motion records was selected from worldwide earthquakes provided by the PEER center, considering a wide range of amplitude, magnitude, epicentral distance, duration, fundamental period, and frequency. Figure 1 shows the response spectra of the 90 motion records. It should be noted that the mean spectrum of these motions is close to the design response spectrum of the US NRC 1.60 [34].
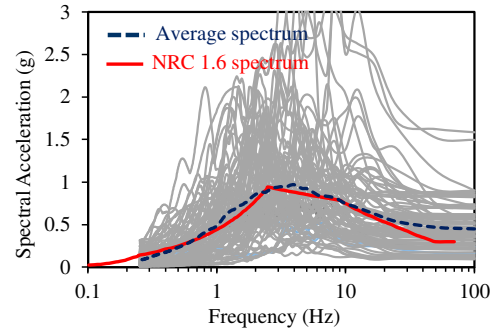
Fig. 1.   Response spectra of 90 motion records.

III. FINITE ELEMENT MODEL OF CONTAINMENT STRUCTURE

The reactor containment structure in the Advanced Power Reactor 1400 (APR-1400) NPP was employed to develop the modeling. This structure is made of reinforced concrete with a cylinder and a top dome. The diameter and height of the cylinder are 47m and 54m respectively. The thickness of the RC cylinder wall is 1.22m. The radius and thickness of the dome are 23.2m and 1.07m respectively. Figure 2 shows the structural dimensions of the containment structure.
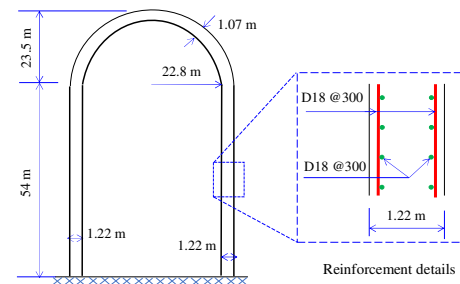
Fig. 2.   Configurations of the containment structure.

Since the containment structure is a vertically symmetric cantilever column, its FEM can be developed using the simplified LMSM. This numerical model was based on beam elements with nodal masses assigned at the nodes of the elements. The model consisted of 14 beam elements, where their length was determined based on the change of vertical stiffness of the structure and the location where secondary systems are connected to the containment structure. The lumped masses and structural section properties of elements were calculated based on the real cross-section of the structure [35]. The LMSM of the containment structure was constructed in SAP2000, a commercial structural analysis program. Figure 3(a) shows the LMSM of the containment structure in SAP2000 and Table II shows the material properties.

3D FEM is known to be the most accurate numerical approach and was used to validate the simplified LMSM. In this study, 3D FEM was developed using solid elements in ANSYS. The structural model was meshed into 13,571 prism elements, after conducting a sensitivity meshing analysis as shown in Figure 3(b). The elastic modulus of the material was 30,500MPa, Poisson's ratio was 0.17, and volumetric density was 24.0KN/m³.

(a) LMSM   (b) 3D FEM
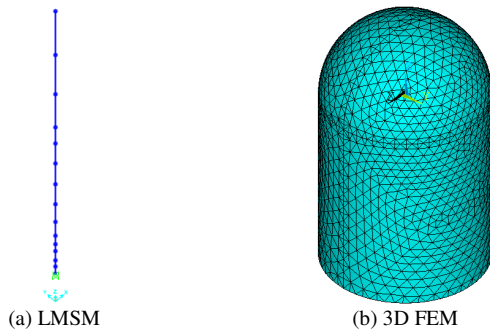
Fig. 3.   Finite element models.

TABLE II.   MATERIAL PROPERTIES USED IN LMSM

Model	Elastic modulus (kN/m²)	Volumetric density (kN/m³)	Poisson's ratio
Containment structure	3.05E+07	0.00	0.170

IV. SEISMIC RESPONSES OF THE CONTAINMENT STRUCTURE

A series of linear time-history analyses was performed since the stiffness of the containment structure was very high and was expected to behave elastically under earthquakes. Acceleration records were imposed on the horizontal direction, and the effects of vertical motion were neglected. The EDPs (seismic responses) of the structure were quantified in terms of floor accelerations and displacements. These parameters are commonly used in structural and earthquake engineering analyses [36-38]. Figure 4 displays the time-history responses of the containment structure at the top and middle nodes using LMSM and 3D FEM, showing that the results of the two models are highly compatible. Figure 5 shows the Floor Response Spectra (FRS) at different elevations of the structure, which also implies that LMSM results are very close to 3D FEM and highlights the capability of the former to perform a seismic time-history analysis of the NPP structure.

V. SEISMIC DEMAND REGRESSION MODEL

The Seismic Demand Regression Model (SDRM) has been widely used to represent the relationship between earthquake IMs and EDPs. This model was also applied to seismic designs according to the probabilistic approach [6, 39]. The popular expression of SDRM is [7, 10, 40]:

$$S_D = a \times (IM)^b \quad (1)$$

where S_D is the mean seismic response of the structure, a and b are regression coefficients, and IM is the intensity measure considered. Equation (1) can be also written as:

$$ln(S_D) = ln(a) + b \times ln(IM) \quad (2)$$
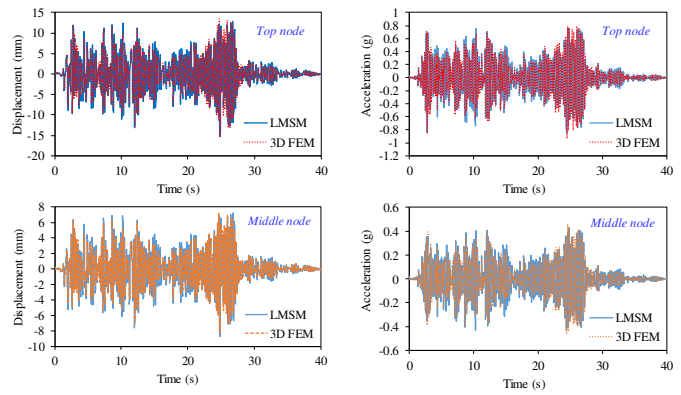
Fig. 4.   Time-history responses of the structure subjected to the 1940 El Centro earthquake.
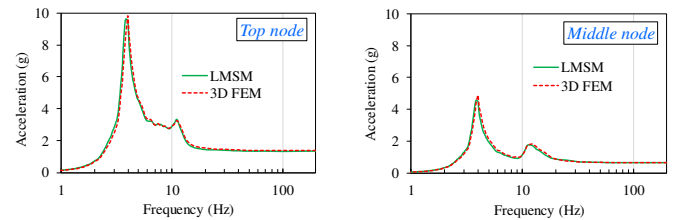
Fig. 5.   FRS at different elevations of the structure under the 1940 El Centro earthquake.

A total of 40 SDRMs of the structure were constructed for 20 IMs and EDPs. Optimal IMs were evaluated using four statistical indicators: coefficient of determination (R^2), efficiency (standard deviation), practicality, and proficiency. It should be noted that R^2 represents the percentage of data closest to the regression line, and a higher R^2 value indicates a more optimal SDRM. On the contrary, efficiency denotes the scattering (standard deviation) of SDRM, and smaller efficiency indicates more optimal SDRMs. It practicality indicates the slope of the regression line, and smaller practicality means more correlated IM. Similarly, proficiency represents the balance between efficiency and practicality, and smaller proficiency means a more proficient SDRM.

Figure 6 shows the SDRMs for floor displacement for the 20 IMs. The results demonstrate that the IMs corresponding to SDRMs with the highest R^2 values and having the smallest scattering were: $S_a(T_1)$, $S_v(T_1)$, $S_d(T_1)$, ASI, EPA, PGA, and $A95$. Displacement-based regression models using $S_a(T_1)$, $S_v(T_1)$, and $S_d(T_1)$ had R^2 greater than 0.95. Similarly, R^2 values were also greater than 0.85 in acceleration-based regression models using $S_a(T_1)$, $S_v(T_1)$, $S_d(T_1)$. The trend of SDRMs was similar for both using floor displacement and acceleration as EDPs. Overall, a high correlation was observed for acceleration-based IMs, attributed to the large mass and stiffness of the investigated structure, so it was sensitive to acceleration rather than velocity and displacement [24]. Moreover, $S_a(T_1)$, $S_v(T_1)$, $S_d(T_1)$ had the strongest correlation with EDPs since they combine the earthquake characteristic and structural property (i.e. the fundamental period T_1).
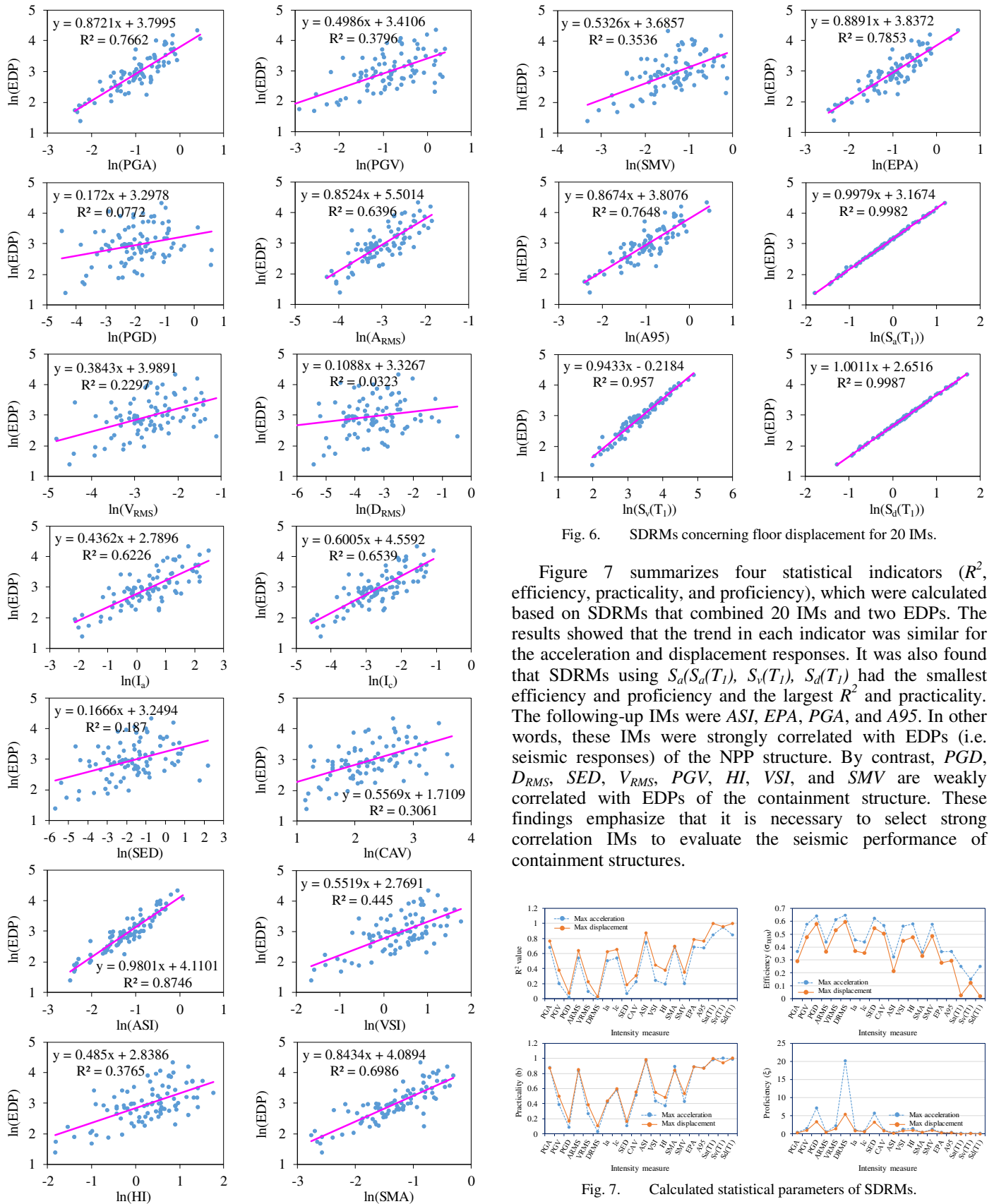
Fig. 6.   SDRMs concerning floor displacement for 20 IMs.

Figure 7 summarizes four statistical indicators (R^2, efficiency, practicality, and proficiency), which were calculated based on SDRMs that combined 20 IMs and two EDPs. The results showed that the trend in each indicator was similar for the acceleration and displacement responses. It was also found that SDRMs using $S_a(S_a(T_1), S_v(T_1), S_d(T_1)$ had the smallest efficiency and proficiency and the largest R^2 and practicality. The following-up IMs were *ASI*, *EPA*, *PGA*, and *A95*. In other words, these IMs were strongly correlated with EDPs (i.e. seismic responses) of the NPP structure. By contrast, *PGD*, D_{RMS}, *SED*, V_{RMS}, *PGV*, *HI*, *VSI*, and *SMV* are weakly correlated with EDPs of the containment structure. These findings emphasize that it is necessary to select strong correlation IMs to evaluate the seismic performance of containment structures.
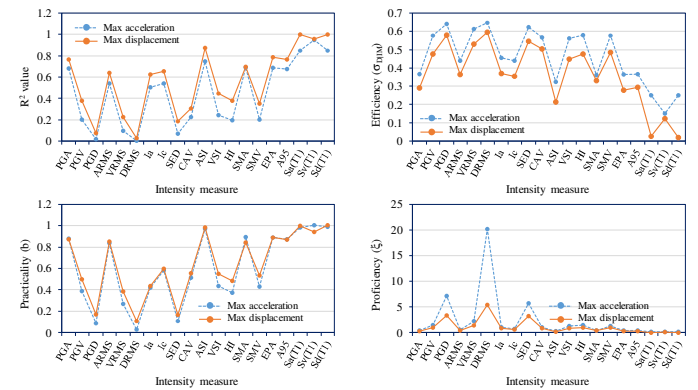
Fig. 7.   Calculated statistical parameters of SDRMs.

VI. CONCLUSION

This study examined the correlation between earthquake IMs and EDPs of the containment structure of an APR-1400 NPP. Numerical modeling was developed using LMSM and validated using a 3D FEM. A set of 90 ground motion records and 20 typical IMs were considered in time-history and correlation analyses. The correlation of IMs with EDPs was evaluated using statistical indicators. Based on the numerical results, the following conclusions can be drawn:

- LMSM is reliable for performing time-history analysis of containment structures in NPPs.

- The strongest correlated IMs with EDPs of the containment structure were $S_a(T_1)$, $S_v(T_1)$, $S_d(T_1)$, followed by *ASI*, *EPA*, *PGA*, and *A95*.

- The weakest correlated IMs with EDPs of the containment structure were *PGD*, D_{RMS}, and *SED*, followed by V_{RMS}, *PGV*, *HI*, *VSI*, and *SMV*.

- It is necessary to select strongly correlated IMs to evaluate the seismic performance and fragility of NPP containment structures.

REFERENCES

[1] A. Elenas and K. Meskouris, "Correlation study between seismic acceleration parameters and damage indices of structures," *Engineering Structures*, vol. 23, no. 6, pp. 698–704, Jun. 2001, https://doi.org/10.1016/S0141-0296(00)00074-2.

[2] V. V. Cao and H. R. Ronagh, "Correlation between seismic parameters of far-fault motions and damage indices of low-rise reinforced concrete frames," *Soil Dynamics and Earthquake Engineering*, vol. 66, pp. 102–112, Nov. 2014, https://doi.org/10.1016/j.soildyn.2014.06.020.

[3] M. Ghayoomi and S. Dashti, "Effect of Ground Motion Characteristics on Seismic Soil-Foundation-Structure Interaction," *Earthquake Spectra*, vol. 31, no. 3, pp. 1789–1812, Aug. 2015, https://doi.org/10.1193/040413EQS089M.

[4] K. Kostinakis, A. Athanatopoulou, and K. Morfidis, "Correlation between ground motion intensity measures and seismic damage of 3D R/C buildings," *Engineering Structures*, vol. 82, pp. 151–167, Jan. 2015, https://doi.org/10.1016/j.engstruct.2014.10.035.

[5] A. Massumi and F. Gholami, "The influence of seismic intensity parameters on structural damage of RC buildings using principal components analysis," *Applied Mathematical Modelling*, vol. 40, no. 3, pp. 2161–2176, Feb. 2016, https://doi.org/10.1016/j.apm.2015.09.043.

[6] J. R. Pejovic, N. N. Serdar, and R. R. Pejovic, "Optimal intensity measures for probabilistic seismic demand models of RC high-rise buildings," *Earthquakes and Structures*, vol. 13, no. 3, pp. 221–230, 2017, https://doi.org/10.12989/eas.2017.13.3.221.

[7] J. E. Padgett, B. G. Nielson, and R. DesRoches, "Selection of optimal intensity measures in probabilistic seismic demand models of highway bridge portfolios," *Earthquake Engineering & Structural Dynamics*, vol. 37, no. 5, pp. 711–725, 2008, https://doi.org/10.1002/eqe.782.

[8] Ö. Avşar and G. Özdemir, "Response of Seismic-Isolated Bridges in Relation to Intensity Measures of Ordinary and Pulselike Ground Motions," *Journal of Bridge Engineering*, vol. 18, no. 3, pp. 250–260, Mar. 2013, https://doi.org/10.1061/(ASCE)BE.1943-5592.0000340.

[9] Y.-Y. Zhang, Y. Ding, and Y.-T. Pang, "Selection of Optimal Intensity Measures in Seismic Damage Analysis of Cable-Stayed Bridges Subjected to Far-Fault Ground Motions," *Journal of Earthquake and Tsunami*, vol. 09, no. 01, Mar. 2015, Art. no. 1550003, https://doi.org/10.1142/S1793431115500037.

[10] V. Jahangiri, M. Yazdani, and M. S. Marefat, "Intensity measures for the seismic response assessment of plain concrete arch bridges," *Bulletin of Earthquake Engineering*, vol. 16, no. 9, pp. 4225–4248, Sep. 2018, https://doi.org/10.1007/s10518-018-0334-8.

[11] C. Zelaschi, R. Monteiro, and R. Pinho, "Critical Assessment of Intensity Measures for Seismic Response of Italian RC Bridge Portfolios," *Journal of Earthquake Engineering*, vol. 23, no. 6, pp. 980–1000, Jul. 2019, https://doi.org/10.1080/13632469.2017.1342293.

[12] B. Wei, Z. Hu, X. He, and L. Jiang, "Evaluation of optimal ground motion intensity measures and seismic fragility analysis of a multi-pylon cable-stayed bridge with super-high piers in Mountainous Areas," *Soil Dynamics and Earthquake Engineering*, vol. 129, Feb. 2020, Art. no. 105945, https://doi.org/10.1016/j.soildyn.2019.105945.

[13] H. N. Phan and F. Paolacci, "Efficient Intensity Measures for Probabilistic Seismic Response Analysis of Anchored Above-Ground Liquid Steel Storage Tanks," in *Conference Proceedings - ASME 2016 Pressure Vessels and Piping Conference*, Vancouver, Canada, Dec. 2016, https://doi.org/10.1115/PVP2016-63103.

[14] Y. Qiu, C. Zhou, and S. A, "Correlation between earthquake intensity parameters and damage indices of high-rise RC chimneys," *Soil Dynamics and Earthquake Engineering*, vol. 137, Oct. 2020, Art. no. 106282, https://doi.org/10.1016/j.soildyn.2020.106282.

[15] Z. Chen and J. Wei, "Correlation between ground motion parameters and lining damage indices for mountain tunnels," *Natural Hazards*, vol. 65, no. 3, pp. 1683–1702, Feb. 2013, https://doi.org/10.1007/s11069-012-0437-5.

[16] D. D. Nguyen, D. Park, S. Shamsher, V. Q. Nguyen, and T. H. Lee, "Seismic vulnerability assessment of rectangular cut-and-cover subway tunnels," *Tunnelling and Underground Space Technology*, vol. 86, pp. 247–261, Apr. 2019, https://doi.org/10.1016/j.tust.2019.01.021.

[17] H. Shakib and V. Jahangiri, "Intensity measures for the assessment of the seismic response of buried steel pipelines," *Bulletin of Earthquake Engineering*, vol. 14, no. 4, pp. 1265–1284, Apr. 2016, https://doi.org/10.1007/s10518-015-9863-6.

[18] D. D. Nguyen, B. Thusa, H. Park, M. S. Azad, and T. H. Lee, "Efficiency of various structural modeling schemes on evaluating seismic performance and fragility of APR1400 containment building," *Nuclear Engineering and Technology*, vol. 53, no. 8, pp. 2696–2707, Aug. 2021, https://doi.org/10.1016/j.net.2021.02.006.

[19] T. K. Mandal, S. Ghosh, and N. N. Pujari, "Seismic fragility analysis of a typical Indian PHWR containment: Comparison of fragility models," *Structural Safety*, vol. 58, pp. 11–19, Jan. 2016, https://doi.org/10.1016/j.strusafe.2015.08.003.

[20] T. T. Tran, A. T. Cao, T. H. X. Nguyen, and D. Kim, "Fragility assessment for electric cabinet in nuclear power plant using response surface methodology," *Nuclear Engineering and Technology*, vol. 51, no. 3, pp. 894–903, Jun. 2019, https://doi.org/10.1016/j.net.2018.12.025.

[21] S. G. Cho and Y. H. Joe, "Seismic fragility analyses of nuclear power plant structures based on the recorded earthquake data in Korea," *Nuclear Engineering and Design*, vol. 235, no. 17, pp. 1867–1874, Aug. 2005, https://doi.org/10.1016/j.nucengdes.2005.05.021.

[22] I. K. Choi, Y. S. Choun, S. M. Ahn, and J. M. Seo, "Seismic fragility analysis of a CANDU type NPP containment building for near-fault ground motions," *KSCE Journal of Civil Engineering*, vol. 10, no. 2, pp. 105–112, Mar. 2006, https://doi.org/10.1007/BF02823928.

[23] C. Li, C. Zhai, S. Kunnath, and D. Ji, "Methodology for selection of the most damaging ground motions for nuclear power plant structures," *Soil Dynamics and Earthquake Engineering*, vol. 116, pp. 345–357, Jan. 2019, https://doi.org/10.1016/j.soildyn.2018.09.039.

[24] D. D. Nguyen, B. Thusa, T. S. Han, and T. H. Lee, "Identifying significant earthquake intensity measures for evaluating seismic damage and fragility of nuclear power plant structures," *Nuclear Engineering and Technology*, vol. 52, no. 1, pp. 192–205, Jan. 2020, https://doi.org/10.1016/j.net.2019.06.013.

[25] S. L. Kramer, *Geotechnical Earthquake Engineering*, 1st edition. Upper Saddle River, NJ, USA: Prentice Hall, 1996.

[26] A. Arias, "Measure of Earthquake Intensity," in *Seismic Design for Nuclear Power Plants.*, Cambridge, MA, USA: Massachusetts Institute of Technology Press, 1970, pp. 438–483.

[27] Y.-J. Park, A. H.-S. Ang, and Y. K. Wen, "Seismic Damage Analysis of Reinforced Concrete Buildings," *Journal of Structural Engineering*, vol. 111, no. 4, pp. 740–757, Apr. 1985, https://doi.org/10.1061/(ASCE) 0733-9445(1985)111:4(740).

[28] J. R. Benjamin, "A Criterion for Determining Exceedances of the Operating Basis Earthquake," Electric Power Research Institute, Palo Alto, CA, USA, ERPI NP-5930, 1988.

[29] J. L. Von Thun, L. H. Roehm, G. A. Scott, and J. A. Wilson, "Earthquake Ground Motions for Design and Analysis of Dams," in *Earthquake Engineering and Soil Dynamics II - Recent Advances in Ground-Motion Evaluation*, Park City, UT, USA, 1988, pp. 463–481.

[30] G. W. Housner, "Spectrum Intensities of Strong-Motion Earthquakes," C. M. Duke and M. Feigen, Eds. Los Angeles: Earthquake Engineering Research Institute, 1952, pp. 20–36.

[31] O. W. Nuttli, "The relation of sustained maximum ground acceleration and velocity to earthquake intensity and magnitude," US Army Waterways Experimental Station, Vicksburg, MS, USA, Misc. Paper S-73-1 16, 1979.

[32] N. Shome, C. A. Cornell, P. Bazzurro, and J. E. Carballo, "Earthquakes, Records, and Nonlinear Responses," *Earthquake Spectra*, vol. 14, no. 3, pp. 469–500, Aug. 1998, https://doi.org/10.1193/1.1586011.

[33] S. K. Sarma and K. S. Yang, "An evaluation of strong motion records and a new parameter A95," *Earthquake Engineering & Structural Dynamics*, vol. 15, no. 1, pp. 119–132, 1987, https://doi.org/10.1002/ eqe.4290150109.

[34] "Design Response Spectra for Seismic Design of Nuclear Power Plants," Nuclear Regulatory Commission, Washington, DC, USA, Regulatory Guide 1.60 - Revision 2 2014–16297, Jul. 2014.

[35] D.-D. Nguyen, T.-H. Lee, and V.-T. Phan, "Optimal Earthquake Intensity Measures for Probabilistic Seismic Demand Models of Base-Isolated Nuclear Power Plant Structures," *Energies*, vol. 14, no. 16, Jan. 2021, Art. no. 5163, https://doi.org/10.3390/en14165163.

[36] D. D. Nguyen and C. N. Nguyen, "Seismic Responses of NPP Structures Considering the Effects of Lead Rubber Bearing," *Engineering, Technology & Applied Science Research*, vol. 10, no. 6, pp. 6500–6503, Dec. 2020, https://doi.org/10.48084/etasr.3926.

[37] J. A. Alomari, "Effect of the Presence of Basements on the Vibration Period and Other Seismic Responses of R.C. Frames," *Engineering, Technology & Applied Science Research*, vol. 9, no. 5, pp. 4712–4717, Oct. 2019, https://doi.org/10.48084/etasr.3005.

[38] P. C. Nguyen, B. Le-Van, and S. D. T. V. Thanh, "Nonlinear Inelastic Analysis of 2D Steel Frames : An Improvement of the Plastic Hinge Method," *Engineering, Technology & Applied Science Research*, vol. 10, no. 4, pp. 5974–5978, Aug. 2020, https://doi.org/10.48084/ etasr.3600.

[39] D.-D. Nguyen, B. Thusa, M. S. Azad, V.-L. Tran, and T.-H. Lee, "Optimal earthquake intensity measures for probabilistic seismic demand models of ARP1400 reactor containment building," *Nuclear Engineering and Technology*, vol. 53, no. 12, pp. 4179–4188, Dec. 2021, https://doi.org/10.1016/j.net.2021.06.034.

[40] C. A. Cornell, F. Jalayer, R. O. Hamburger, and D. A. Foutch, "Probabilistic Basis for 2000 SAC Federal Emergency Management Agency Steel Moment Frame Guidelines," *Journal of Structural Engineering*, vol. 128, no. 4, pp. 526–533, Apr. 2002, https://doi.org/ 10.1061/(ASCE)0733-9445(2002)128:4(526).